The Astrophysical Journal, 770:158 (6pp), 2013 June 20 doi:10.1088/0004-637X/770/2/158

GEMINI SPECTROSCOPY OF ULTRACOMPACT DWARFS IN THE FOSSIL GROUP NGC 1132

Juan P. Madrid[1] and Carlos J. Donzelli[2,3]
[1] Centre for Astrophysics and Supercomputing, Swinburne University of Technology, Hawthorn, VIC 3122, Australia
[2] Instituto de Investigaciones en Astronomía Teórica y Experimental IATE, Observatorio Astronómico de Córdoba, Laprida 854, X5000BGR, Córdoba, Argentina
[3] Consejo Nacional de Investigaciones Científicas y Técnicas (CONICET), Avenida Rivadavia 1917, C1033AAJ, Buenos Aires, Argentina
Received 2013 February 28; accepted 2013 May 4; published 2013 June 6

ABSTRACT

A spectroscopic follow-up of ultracompact dwarf (UCD) candidates in the fossil group NGC 1132 is undertaken with the Gemini Multi Object Spectrograph. These new Gemini spectra prove the presence of six UCDs in the fossil group NGC 1132 at a distance of $D \sim 100$ Mpc and a recessional velocity of $v_r = 6935 \pm 11$ km s^{-1}. The brightest and largest member of the UCD population is an M32 analog with a size of 77.1 pc and a magnitude of $M_V = -14.8$ mag with the characteristics in between those of the brightest UCDs and compact elliptical galaxies. The ensemble of UCDs have an average radial velocity of $\langle v_r \rangle = 6966 \pm 208$ km s^{-1} and a velocity dispersion of $\sigma_v = 169 \pm 18$ km s^{-1} similar to the one of poor galaxy groups. This work shows that UCDs can be used as test particles to determine the dynamical properties of galaxy groups. The presence of UCDs in the fossil group environment is confirmed and thus the fact that UCDs can form across diverse evolutionary conditions.

Key words: galaxies: clusters: general – galaxies: dwarf – galaxies: elliptical and lenticular, cD – galaxies: groups: general – galaxies: star clusters: general

Online-only material: color figures

1. INTRODUCTION

Ultracompact dwarfs (UCDs) are compact stellar systems with characteristics between those of globular clusters and compact elliptical galaxies, particularly with sizes between 10 and 100 pc. UCDs were discovered in the Fornax cluster (Hilker et al. 1999; Drinkwater et al. 2000). Subsequent searches in other galaxy clusters revealed that, far from being an oddity to Fornax, UCDs were present in all major galaxy clusters in the nearby universe (Brüns & Kroupa 2012 and their comprehensive set of references therein).

In recent years, several studies have searched for UCDs in environments other than galaxy clusters. New UCDs have been found in low-density environments (Hau et al. 2009), galaxy groups (Romanowsky et al. 2009), and field galaxies (Norris & Kannappan 2011). Within this framework, and through the analysis of Advanced Camera for Surveys (ACS) imaging, Madrid (2011) found 11 UCDs and 39 extended star cluster candidates associated with the fossil group NGC 1132. These objects were identified through the analysis of their colors, luminosity, and structural parameters.

Fossil groups are galaxy systems where a luminous early-type galaxy is brighter than any other group member by more than two magnitudes. This dominant galaxy is believed to be the end product of the merger of a galaxy group into a single entity (Ponman et al. 1994). Fossil groups have X-ray luminosities comparable to galaxy groups but a characteristic absence of $L^\star$ galaxies (Jones et al. 2003). Analysis of numerical simulations shows that fossil groups had an early assembly and a passive evolution thereafter (e.g., Díaz-Giménez et al. 2011). The surface brightness profile and the globular cluster system of the fossil group NGC 1132 were studied by Alamo-Martínez et al. (2012). These authors find that both surface brightness and specific frequency of globular clusters ($S_N = 3.1 \pm 0.3$) in NGC 1132 are similar to those of normal elliptical galaxies.

Of the 11 UCD candidates found by Madrid (2011), 9 share the same parameter space as the brightest globular clusters in the color–magnitude diagram (CMD) of the NGC 1132 globular cluster system. One UCD candidate, which will be designated as UCD1, is almost four magnitudes brighter than the brightest globular cluster associated with NGC 1132. UCD1 is 6.6 kpc from the center of NGC 1132, has a half-light radius of 77.1 pc, and a magnitude of $m_{F850LP} = 18.49$ mag. A second UCD candidate, for which a spectrum was also obtained, had particularly blue colors compared to the most luminous globular clusters.

The characteristics of UCD1 make it an interesting object since it is the link between the most massive UCDs found so far and the lowest mass M32-like galaxies. UCD1 is the brightest object in a recent compilation of 813 UCDs and extended objects (Brüns & Kroupa 2012). Indeed, high surface brightness compact elliptical galaxies or M32-like stellar systems are rare. Chilingarian & Mamon (2008) list only six confirmed stellar systems similar to M32.

As pointed out recently by Brüns & Kroupa (2012), only one-fifth of all published UCDs have been so far spectroscopically confirmed. In this work, we present the results of an observing campaign with Gemini North to obtain spectroscopic follow-up of UCD candidates in the fossil group NGC 1132 presented by Madrid (2011).

2. OBSERVATIONS

Spectra for seven UCD candidates and the brightest globular cluster in the fossil group NGC 1132 were obtained with the Gemini North telescope using the Gemini Multi Object Spectrograph (GMOS). These observations were acquired under program GN-2012B-Q-10. UCD candidates were determined through the analysis of *Hubble Space Telescope* (*HST*) imaging. A multislit mask was created using a pre-image provided by Gemini. Given that the ACS on board *HST* has a field of view of 202 × 202 arcsec, all targets are located within this small area centered on the host galaxy. The central concentration limited the total number of targets that fit on the GMOS slit mask.

The spectroscopic data were acquired in queue mode on 2012 September 20 using a multislit mask. Individual slits had a width of 1 arcsec. The grating in use was the B600+_G5323 that has

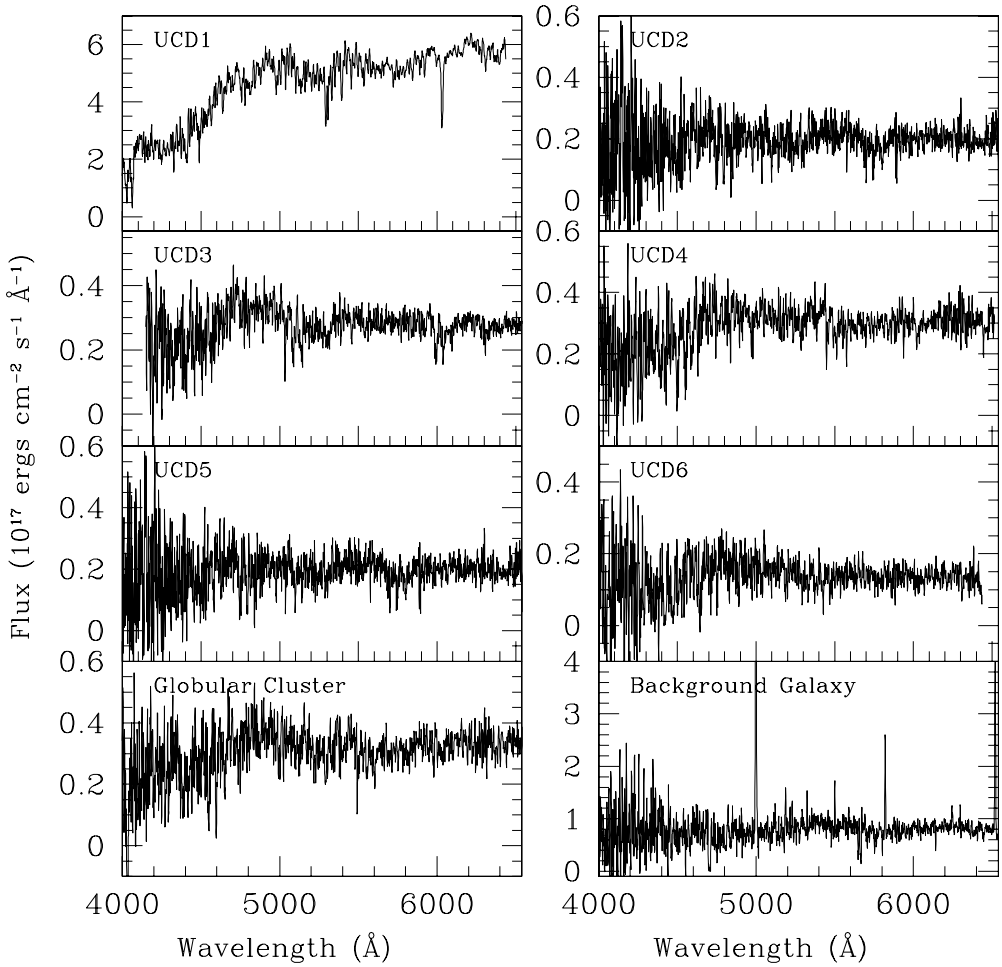

Figure 1. Calibrated Gemini/GMOS spectra of six confirmed UCDs, one globular cluster, and a background galaxy in the NGC 1132 field. The most prominent lines of these spectra, particularly UCD1, are the magnesium and sodium doublets with rest-frame wavelengths of 5169, 5175 Å and 5890, 5896 Å, respectively. Note that these spectra are not corrected for radial velocities.

a ruling density of 600 lines mm^{-1}. Three exposures of 1800 s each were obtained with the central wavelengths of 497 and 502 nm. Two additional exposures of 1800 s each were obtained with a central wavelength of 507 nm. Science targets thus have a total exposure time of ∼4 hr. Flatfields, spectra of the standard star BD +28°4211, and the copper–argon CuAr lamp were also acquired to perform flux calibration. A binning of 2 × 2 was used, yielding a scale of 0.1456 arcsec pixel^{-1} and a theoretical dispersion of ∼0.9 Å pixel^{-1}. Our targets transit ∼30° from the zenith and if the position angle is set to 90°, the displacement due to atmospheric refraction is small in our configuration. Slit losses due to atmospheric refraction can be neglected.

3. DATA REDUCTION AND ANALYSIS

All science and calibration files were retrieved from the Gemini Science Archive hosted by the Canadian Astronomy Data Center. The data reduction described below was carried out with the Gemini IRAF package. Flatfields were derived with the task GSFLAT and the flatfield exposures. Spectra were reduced using GSREDUCE, this does a standard data reduction, that is, performs bias, overscan, and cosmic-ray removal as well as applying the flatfield derived with GSFLAT. GMOS-North detectors are read with six amplifiers and generate files with six extensions. The task GMOSAIC was used to generate data files with a single extension. The sky level was removed interactively using the task GSKYSUB and the spectra were extracted using GSEXTRACT.

Flux calibration was performed using the spectra of the standard star BD +28°4211, acquired with an identical instrument configuration. Spectra of CuAr lamps were obtained immediately after the science targets were observed and were used to achieve wavelength calibration using the task GSWAVELENGTH. We use GSTRANSFORM to rectify, interpolate, and calibrate the spectra using the wavelength solution found by GSWAVELENGTH. The sensitivity function of the instrument was derived using GSSTANDARD and the reference file for BD +28°4211 provided by Gemini observatory. Science spectra were flux calibrated with GSCALIBRATE which uses the sensitivity function derived by GSSTANDARD.

4. RESULTS

Figure 1 presents the calibrated spectra of six UCDs, the brightest globular cluster of the NGC 1132 globular cluster system, and a background galaxy thought to be a UCD with particularly blue colors. Various absorption lines are identifiable in the spectra of UCDs, particularly in the spectrum of UCD1 which has a higher signal-to-noise ratio. The two most prominent absorption features in the spectrum of UCD1 are the magnesium and sodium doublets with rest-frame wavelengths of 5169, 5175 Å and 5890, 5896 Å, respectively. These two

Table 1
Lick Indices for UCD1

Hβ	HδA	HγA	Mgb	Fe 5270	Fe 5335	⟨Fe⟩	[MgFe]
1.96 ± 0.02	−1.92 ± 0.15	−7.69 ± 0.15	5.03 ± 0.02	3.57 ± 0.02	1.86 ± 0.01	2.7 ± 0.02	3.1 ± 0.03

doublets are also evident in the UCD spectra published by Francis et al. (2012). Other lines present in the spectrum of UCD1 are Ca and Fe (5269 Å), Fe (5331 Å; 4384 Å), He II (5411 Å), Hβ (4861 Å), and Ca I (4227 Å).

4.1. Redshift Determination

The redshift of the targets is derived using the IRAF task FXCOR that computes radial velocities by deriving the Fourier cross-correlation between two spectra. As a reference spectrum, we use data of the Galactic globular cluster BH 176 taken in the same GMOS configuration during a previous Gemini run (Davoust et al. 2011). For UCD1, the task FXCOR returns a radial velocity of 7158 ± 32 km s^{-1}. The host galaxy NGC 1132 has a published radial velocity of 6935 ± 11 km s^{-1} (Collobert et al. 2006). With these results we confirm that UCD1 is located within the fossil group NGC 1132 at a redshift of $z \sim 0.023$. This redshift measurement validates the photometric and structural parameters derived by Madrid (2011) for UCD1.

4.2. Age and Metallicity of UCD1, an M32-like Object

A caveat for this section is relevant: an accurate age and metallicity determination of the old stellar systems studied here is difficult. In a similar spectroscopic study of UCDs, Francis et al. (2012) derived the ages of 21 UCDs using both Lick indices and spectral fitting of simple stellar populations and the results of these two techniques do not correlate with one another. The metallicities of these 21 UCDs, also derived by Francis et al. (2012), have better uncertainties and show a correlation between the two methods with an offset of 0.2 dex.

The stellar population synthesis code STARLIGHT (Cid Fernandes et al. 2005) was used with the aim of deriving the metallicity of UCD1. STARLIGHT compared the Gemini spectrum of UCD1 with a database of 150 spectral templates and found that the best fit is provided by a combination of two stellar populations: one representing 30% of the flux and having solar metallicity ($Z = 0.02$) and a second population accounting for 70% of the flux and having supersolar metallicity ($Z = 0.05$). This spectral fitting also yields an age of 13 Gyr for UCD1.

For spectra with sufficient signal-to-noise Lick indices (Worthey et al. 1994) can be derived. The code GONZO (Puzia et al. 2002) was used to derive Lick indices for UCD1 which is the only UCD with enough signal to generate significant results. The Gemini spectrum is degraded to the Lick resolution by GONZO. We also apply the zero points of the calibration given by Loubser et al. (2009). The values for the lick indices and their associated Poisson errors are given in Table 1; this allows comparison with existent and future studies. By comparing the indices ⟨Fe⟩ and Mgb to the single stellar population models of Thomas et al. (2003), we can derive an α-element abundance for UCD1 of [α/Fe] = +0.3. Indices Hβ = 1.96 Å and Fe 5270 = 3.57 Å of UCD1 are very similar to the values derived by Chiboucas et al. (2011) for UCD 121666 in the Coma cluster. UCD 121666 has an Hβ = 1.84 Å and Fe 5270 = 3.48 Å.

The Lick indices we obtained were given as input to the publicly available code EZ Ages (Graves & Schiavon 2008). This code determines ages and abundances of unresolved stellar populations using their Lick indices. We chose an alpha-enhanced isochrone fitting and found an age of 7.5 Gyr and an iron abundance of [Fe/H] = −0.17. The chemical abundances of Grevesse & Sauval (1998) yield a metallicity of $Z = 0.015$. The metallicity derived for UCD1 is high among UCDs but not unprecedented (Chiboucas et al. 2011; Francis et al. 2012).

4.3. Internal Velocity Dispersion

The main objective of this work is to obtain redshifts for the UCD candidates. Determining their internal velocity dispersion, roughly of a few tens of kilometers per second, is beyond the resolution of these Gemini/GMOS observations. The empirical spectral resolution of our observations has an FWHM ∼ 200 km s^{-1} at 5000 Å, that is, about 10 times the value of published internal velocity dispersion of UCDs (e.g., $\sigma_v = 20.0$ km s^{-1}; Hasegan et al. 2005).

4.4. UCD Population in the Fossil Group NGC 1132

The redshifts derived with these new Gemini spectra confirm six UCD candidates as true members of the fossil group NGC 1132. The redshifts, photometric, and structural parameters of these UCDs are listed in Table 2. UCD2 through UCD6 are the extension to higher luminosities and redder colors of the brightest globular clusters of NGC 1132. The sizes of UCD2 through UCD6 range between 9.9 and 19.8 pc and all globular clusters have a size smaller than ∼8 pc. The CMD of the NGC 1132 globular cluster system is plotted in Figure 2. This CMD also contains the colors and magnitudes of UCD candidates and objects with spectroscopic data.

These six UCDs have an average radial velocity of $\langle v_r \rangle$ = 6966 ± 208 km s^{-1}. The velocity dispersion of this family of UCDs is σ = 169 ± 18 km s^{-1}, which is in the range of poor galaxy groups, as discussed below. The velocity dispersion was derived, through bootstrapping, using the prescriptions of Strader et al. (2011, their Equation (4)). UCDs can be used in the same manner as globular clusters and planetary nebulae have been used to trace the dynamics of nearby galaxies (e.g., Coccato et al. 2009).

4.5. A Blue UCD Candidate

In Madrid (2011), a particularly "blue" UCD candidate was reported. This UCD candidate satisfied all selection criteria based on size, ellipticity, magnitude, and color. This candidate was the bluest UCD candidate and seemingly did not follow the mass–metallicity relation of massive globular clusters ($M > 10^6 M_\odot$; Bailin & Harris 2009). A Gemini-GMOS spectrum of this object reveals that it is actually a background star-forming galaxy with strong emission lines. This object is represented by a cross on the CMD in Figure 2. Madrid (2011) showed that UCDs have, on average, redder colors than extended globular clusters.

4.6. Spatial Distribution of UCDs

The spatial distribution of globular clusters, UCD candidates, and UCDs with spectroscopic confirmation is presented in

Table 2
Radial Velocities, Photometric, and Structural Parameters

ID	R.A.	Decl.	Radial Velocity	m_{F850LP}	M_{F850LP}	Color	r_h (pc)	R_{GC} (kpc)
UCD1	$2^h52^m51^s$	$-1°16'19''$	7158 ± 32	18.5	−16.4	2.28	77.1	6.6
UCD2	$2^h52^m54^s$	$-1°17'39''$	6834 ± 84	21.0	−13.9	2.12	13.3	36.0
UCD3	$2^h52^m59^s$	$-1°14'54''$	7082 ± 69	21.5	−13.4	1.89	19.8	65.5
UCD4	$2^h52^m52^s$	$-1°15'43''$	6627 ± 60	21.5	−13.3	1.92	16.7	21.7
UCD5	$2^h52^m55^s$	$-1°17'19''$	6949 ± 120	21.9	−13.0	1.92	13.0	32.3
UCD6	$2^h52^m51^s$	$-1°16'06''$	7147 ± 140	22.2	−12.7	1.80	9.9	12.0
GC1	$2^h52^m53^s$	$-1°16'34''$	6948 ± 99	21.7	−13.2	1.75	...	5.6

Notes. Column 1: identifier; Column 2: right ascension; Column 3: declination; Column 4: radial velocity; Column 5: apparent magnitude in the *HST* filter *F850LP* (similar to Sloan *z*); Column 6: absolute magnitude; Column 7: color ($F474W - F850LP$); Column 8: effective radius in parsecs. The size of GC1 is below the resolution limit of *HST*, in this case ∼8 pc in radius; Column 9: projected distance to the center of NGC 1132, in kpc.

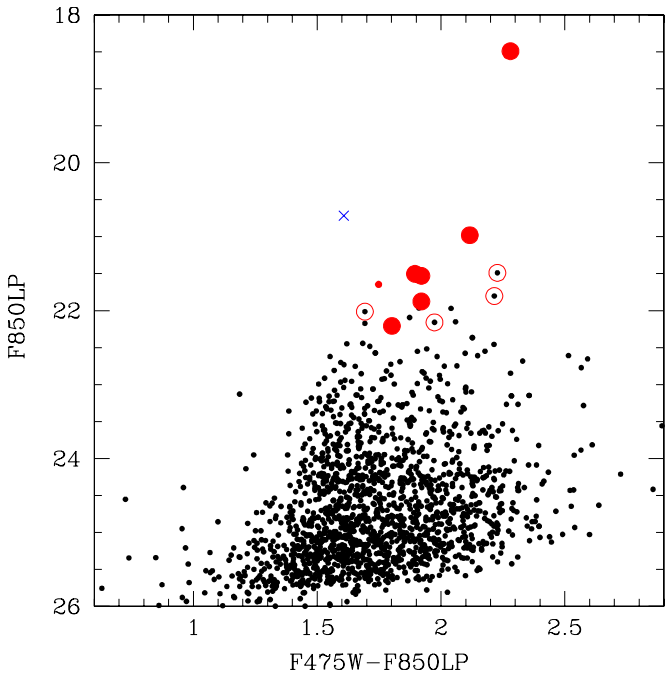

Figure 2. Color–magnitude diagram (CMD) of the globular cluster system of NGC 1132 (black dots). UCD candidates are represented as open red circles. Objects with membership to NGC 1132 confirmed with the Gemini data presented in this paper are displayed as solid red circles. The small red point is GC1. The blue cross represents a background galaxy that masqueraded as an UCD candidate with blue colors in the *HST* images. This CMD was originally derived and presented by Madrid (2011). A detailed analysis of the globular cluster system of NGC 1132 is given by Alamo-Martínez et al. (2012).

(A color version of this figure is available in the online journal.)

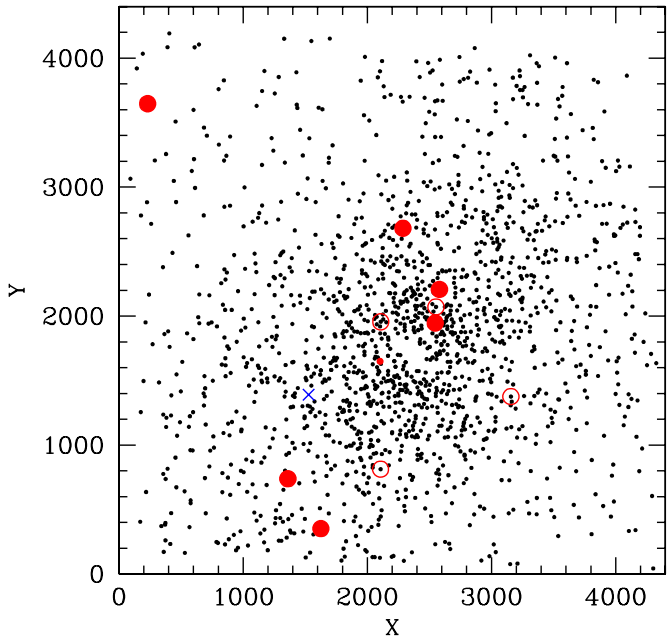

Figure 3. Spatial distribution of globular clusters (black dots), UCD candidates (open red circles), and UCDs with spectroscopic confirmation (solid red circles). The small red dot is GC1. The background galaxy with photometric properties indistinguishable from UCD candidates is represented by a blue cross. This figure represents the field of view of the Advanced Camera for Surveys that, at the distance of NGC 1132, corresponds to ∼100 × 100 kpc.

(A color version of this figure is available in the online journal.)

Figure 3. Both globular clusters and UCDs appear to follow the same spatial distribution. UCDs and globular clusters aggregate toward the center of the host galaxy as is expected for these satellite systems. There is no other particular clustering or alignment of these objects in the ACS field. The projected galactocentric distances of UCDs are given in Table 2. At 6.6 kpc, UCD1 is the closest UCD to the center of NGC 1132.

5. DISCUSSION

5.1. Properties of the Fossil Group NGC 1132

Mulchaey & Zabludoff (1999) call for the use of dwarf galaxies as test particles for the study of the dynamics and dark matter halo of NGC 1132. UCDs can fulfill this role. In galaxy groups $M^\star$ galaxies are expected to merge in a fraction of a Hubble time while, on the other hand, dwarf galaxies have dynamical friction timescales greater than a Hubble time (Mulchaey & Zabludoff 1999). Albeit based on a small sample, the velocity dispersion of the UCD population can be used in existing scaling relations for the X-ray luminosity and group richness.

Several studies have derived a relation between X-ray luminosity (L_X) and velocity dispersion σ_v of galaxy clusters (Ortiz-Gil et al. 2004 and references therein), and galaxy groups (Xue & Wu 2000). Whether fossil galaxy groups follow the same scaling relations of galaxy clusters or have a shallower $L_X \propto \sigma_v$ relation is still a matter of debate (Khosroshahi et al. 2007).

A relation between X-ray luminosity (L_X) and velocity dispersion σ_v for galaxy groups is $L_X = 10^{-2.95\pm0.30}\sigma_v^{1.00\pm0.12}$ in units of 10^{42} erg s^{-1} (Xue & Wu 2000). If we insert the value

for the velocity dispersion of UCDs, $\sigma_v = 169$ km s^{-1}, in the above formula the X-ray luminosity is $L_X = 0.2 \times 10^{42}$. This value is more than a factor of 10 lower than the value reported by Mulchaey & Zabludoff (1999) of $\sim 2.5 \times 10^{42}\, h_{100}^{-2}$ erg s^{-1}. A better match to the observation is given by the relation between L_X and σ for galaxy clusters derived by Ortiz-Gil et al. (2004). These authors give the following relation for what they call a volume-limited sample: $L_X = 10^{35.16\pm0.09}\sigma^{3.2\pm0.3}$. This formula yields $L_X = 1.9 \times 10^{42}$ erg s^{-1}, which is a better approximation to the observed value. In a recent work, Connelly et al. (2012) make a detailed analysis of a sample of galaxy groups and give L_X–σ relations that depend on different factors, for instance, number of group members and radial cuts applied. One of the Connelly et al. (2012) relations yields an X-ray luminosity of $L_X \sim 3 \times 10^{43}$ erg s^{-1}. There is a discrepancy between the different L_X–σ relations published in previous studies.

Pisani et al. (2003) derived a correlation between group richness, or the number of group members (N), and velocity dispersion (σ_v): $\log N = 127 \log \sigma_v - 1.47$. If the velocity dispersion of UCDs are indicative of the primordial velocity dispersion of NGC 1132, according to the Pisani et al. (2003) formula the UCD population has the velocity dispersion corresponding to a poor group with $N = 22$ members.

Mendes de Oliveira & Carrasco (2007) report the velocity dispersion of, among other objects, two Hickson Compact Groups (HCGs) at low redshift: HCG 31 has a velocity dispersion of $\sigma_v = 60$ km s^{-1} and HCG 79 has a velocity dispersion of $\sigma_v = 138$ km s^{-1}. At $\sigma_v = 169$ km s^{-1}, the velocity dispersion of NGC 1132 is higher than these two low-redshift compact groups but lower than the average $\sigma_v = 300$ km s^{-1} found for a collection of 20 groups by Mahdavi et al. (1999).

5.2. UCDs in Different Environments

Analysis of high-resolution *HST* data is a very efficient method to discover UCDs in very diverse environments. The combined study of luminosity, colors, and structural parameters, possible with high-resolution imaging data, yields UCD candidates with very high spectroscopic confirmation rates as shown in this work and in the study of the Coma cluster (Madrid et al. 2010; Chiboucas et al. 2011) among others. Searching for UCDs with seeing-limited data is a more arduous and unfruitful task (e.g., Evstigneeva et al. 2007). One drawback of *HST* detectors is their small field of view that only covers the innermost regions of host galaxies where the strongest tidal effects take place. This work along with the publications cited in the Introduction show that UCDs can be formed in environments with different evolutionary histories.

A historical scarcity of compact stellar systems with characteristic scale sizes between 30 and 100 pc created an unmistakable gap in size–magnitude relations between dwarf ellipticals, compact ellipticals, and globular clusters. Gilmore et al. (2007) have interpreted the gap in the parameter space defined by compact stellar systems as a sign of two distinct families of objects, reflecting the intrinsic properties of dark matter. Globular clusters would belong to a family of dark-matter-free stellar systems while dwarf spheroidals and compact ellipticals form the branch where dark matter is present or even dominant. Gilmore et al. (2007) postulate that dark matter halos have cored mass distributions with characteristic scale sizes of more than 100 pc. UCD1, however, with an effective radius of 77.1 pc is precisely in this gap of compact stellar systems. The brightest UCDs are the ideal candidates to bridge the gap between compact ellipticals and globular clusters. Part of the gap is due to artificial selection effects introduced to eliminate contaminants in photometric studies. For instance, in the ACS Virgo Cluster Survey, an upper limit of 10 pc was imposed on globular cluster candidates. Recent reanalysis of data lifting the 10 pc upper limit on size for compact stellar systems have uncovered new systems previously ignored (e.g., Brodie et al. 2011 for the case of M87).

UCDs are believed to be the bright and massive tail of the globular cluster luminosity function (Drinkwater et al. 2000) or the nuclei of stripped dwarf galaxies (Bekki et al. 2003). A combination of both formation mechanisms has also been proposed (Da Rocha et al. 2011). The large magnitude gap between UCD1 and the brightest globular clusters of NGC 1132 suggests that UCD1 is the leftover core of a spiral galaxy (Bekki et al. 2001). The other UCDs can be stripped dE nuclei or massive globular clusters. The analysis of a large sample of spectroscopic properties of UCDs would prove a link between their stellar populations and those of dwarf galaxies and/or globular clusters.

Based on observations obtained at the Gemini Observatory, which is operated by the Association of Universities for Research in Astronomy, Inc., under a cooperative agreement with the NSF on behalf of the Gemini partnership: the National Science Foundation (United States); the Science and Technology Facilities Council (United Kingdom); the National Research Council (Canada); CONICYT (Chile); the Australian Research Council (Australia); Ministério da Ciência, Tecnologia e Inovação (Brazil); and Ministerio de Ciencia, Tecnología e Innovación Productiva (Argentina). The Gemini data for this paper were obtained under program GN-2012B-Q-10.

We thank the referee for a prompt report with several comments that helped to improve this paper. J. Madrid is grateful for a travel grant from the Australian Nuclear Science and Technology Organization (ANSTO). The access to major research facilities is supported by the Commonwealth of Australia under the International Science Linkages Program. Many thanks to V. Pota, J. Hurley, J. Cooke, E. Caris, A. Hou, P. Jensen, and L. Vega for enlightening discussions. This research has made use of the NASA Astrophysics Data System bibliographic services (ADS), the NASA/IPAC Extragalactic Database (NED), the SIMBAD database, and Google.

Facilities: Gemini:Gillett, *HST*(ACS)

REFERENCES

Alamo-Martínez, K. A., West, M. J., Blakeslee, J. P., et al. 2012, A&A, 546, 15
Bailin, J., & Harris, W. E. 2009, ApJ, 695, 1082
Bekki, K., Couch, W. J., Drinkwater, M. J., & Gregg, M. D. 2001, ApJL, 557, L39
Bekki, K., Couch, W. J., Drinkwater, M. J., & Shioya, Y. 2003, MNRAS, 344, 399
Brodie, J. P., Romanowsky, A. J., Strader, J., & Forbes, D. A. 2011, AJ, 142, 199
Brüns, R. C., & Kroupa, P. 2012, A&A, 547, 65
Chiboucas, K., Tully, R. B., Marzke, R. O., et al. 2011, ApJ, 737, 86
Chilingarian, I. V., & Mamon, G. A. 2008, MNRAS, 385, L83
Cid Fernandes, R., Mateus, A., Sodré, L., Stasinzka, G., & Gomes, J. M. 2005, MNRAS, 358, 363
Coccato, L., Gerhard, O., Arnaboldi, M., et al. 2009, MNRAS, 394, 1249
Collobert, M., Sarzi, M., Davies, R. L., Kuntschner, H., & Colless, M. 2006, MNRAS, 370, 1213
Connelly, J. L., Wilman, D. J., Finoguenov, A., et al. 2012, ApJ, 756, 139
Da Rocha, C., Mieske, S., Georgiev, I. Y., et al. 2011, A&A, 525, 86
Davoust, E., Sharina, M. E., & Donzelli, C. J. 2011, A&A, 528, 70
Díaz-Giménez, E., Zandivarez, A., Proctor, R., Mendes de Oliveira, C., & Abramo, L. R. 2011, A&A, 527, A129

Drinkwater, M. J., Jones, J. B., Gregg, M. D., & Phillipps, S. 2000, PASA, 17, 227
Evstigneeva, E. A., Drinkwater, M. J., Jurek, R., et al. 2007, MNRAS, 378, 1036
Francis, K. J., Drinkwater, M. J., Chilingarian, I. V., Bolt, A. M., & Firth, P. 2012, MNRAS, 425, 325
Gilmore, G., Wilkinson, M. I., Wyse, R. F. G., et al. 2007, ApJ, 663, 948
Graves, G., & Schiavon, R. P. 2008, ApJS, 177, 446
Grevesse, N., & Sauval, A. J. 1998, SSRv, 85, 161
Hasegan, M., Jordán, A., Côté, P., et al. 2005, ApJ, 627, 203
Hau, G. K., Spitler, L. R., Forbes, D. A., et al. 2009, MNRAS, 394, L97
Hilker, M., Infante, L., Vieira, G., Kissler-Patig, M., & Richtler, T. 1999, A&AS, 134, 75
Jones, L. R., Ponman, T. J., Horton, A., et al. 2003, MNRAS, 343, 627
Khosroshahi, H. G., Ponman, T. J., & Jones, L. R. 2007, MNRAS, 377, 595
Loubser, S. I., Sánchez-Blásquez, P., Sansom, A. E., & Soechting, I. K. 2009, MNRAS, 398, 133
Madrid, J. P. 2011, ApJL, 737, L13
Madrid, J. P., Graham, A. W., Harris, W. E., et al. 2010, ApJ, 722, 1707
Mahdavi, A., Geller, M. J., Bohringer, H., Kurtz, M. J., & Ramella, M. 1999, ApJ, 518, 69
Mendes de Oliveira, C. L., & Carrasco, E. R. 2007, ApJL, 670, L93
Mulchaey, J. S., & Zabludoff, A. I. 1999, ApJ, 514, 133
Norris, M. A., & Kannappan, S. J. 2011, MNRAS, 414, 739
Ortiz-Gil, A., Guzzo, L., Schuecker, P., Böringer, H., & Collins, C. A. 2004, MNRAS, 348, 325
Pisani, A., Ramella, M., & Geller, M. 2003, AJ, 126, 1677
Ponman, T. J., Allan, D. J., Jones, L. R., et al. 1994, Natur, 369, 462
Puzia, T. H., Zepf, S. E., Kissler-Patig, M., et al. 2002, A&A, 391, 453
Romanowsky, A. J., Strader, J., Spitler, L. R., et al. 2009, AJ, 137, 4956
Strader, J., Romanowsky, A. J., Brodie, J. P., et al. 2011, ApJS, 197, 33
Thomas, D., Maraston, C., & Bender, R. 2003, MNRAS, 339, 897
Worthey, G., Faber, S. M., Gonzalez, J. J., & Burstein, D. 1994, ApJS, 94, 687
Xue, Y.-J., & Wu, X.-P. 2000, ApJ, 538, 65